Photochemical dissolution of buoyant microplastics to dissolved organic carbon: Rates and microbial impacts

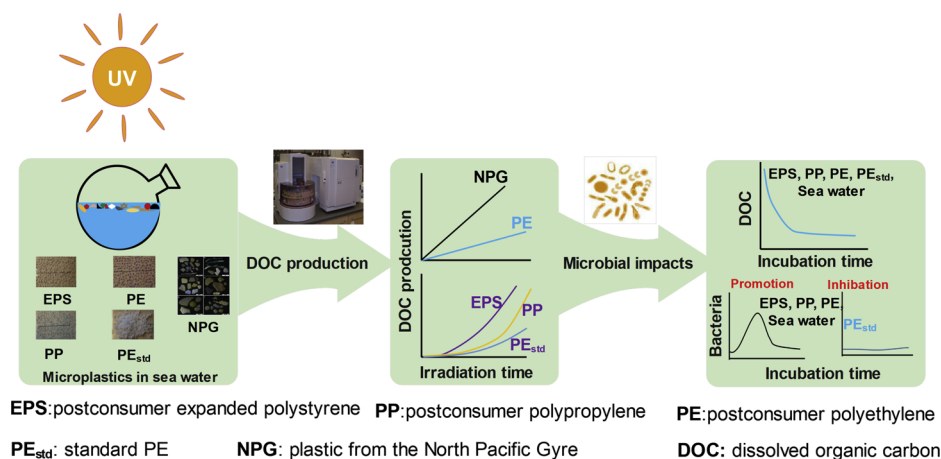Lixin Zhu[a,1,2], Shiye Zhao[b,1,3], Thais B. Bittar[c,2], Aron Stubbins[d,*,2], Daoji Li[a,*]

[a] State Key Laboratory of Estuarine and Coastal Research, East China Normal University, Shanghai, 200241, China
[b] Harbor Branch Oceanographic Institute, Florida Atlantic University, Fort Pierce, Florida 34946, USA.
[c] Marine Science Center, Northeastern University, 430 Nahant Rd, Nahant, MA, 01908, USA
[d] Departments of Marine and Environmental Sciences, Civil and Environmental Engineering, and Chemistry and Chemical Biology, Northeastern University, Boston, MA, 02115, USA

GRAPHICAL ABSTRACT

EPS:postconsumer expanded polystyrene   **PP**:postconsumer polypropylene   **PE**:postconsumer polyethylene

PE_std: standard PE   **NPG**: plastic from the North Pacific Gyre   **DOC**: dissolved organic carbon

ARTICLE INFO

ABSTRACT

Trillions of plastic fragments are afloat at sea, yet they represent only 1–2% of the plastics entering the ocean annually. The fate of the missing plastic and its impact on marine life remains largely unknown. To address these unknowns, we irradiated post-consumer microplastics (polyethylene, PE; polypropylene, PP; and expanded polystyrene, EPS), standard PE, and plastic-fragments collected from the surface waters of the North Pacific Gyre under a solar simulator. We report that simulated sunlight can remove plastics from the sea surface. Simulated sunlight also fragmented, oxidized, and altered the color of the irradiated polymers. Dissolved organic carbon (DOC) is identified as a major byproduct of sunlight-driven plastic photodegradation. Rates of removal depended upon polymer chemistry with EPS degrading more rapidly than PP, and PE being the most photo-resistant polymer studied. The DOC released as most plastics photodegraded was readily utilized by marine bacteria.

* Corresponding authors.
 E-mail addresses: lixinzhu0305@hotmail.com (L. Zhu), shiyezhao@gmail.com (S. Zhao), t.bittar@northeastern.edu (T.B. Bittar),
a.stubbins@northeastern.edu (A. Stubbins), daojili@sklec.ecnu.edu.cn (D. Li).
 [1] These authors contributed equally to this work.
 [2] Skidaway Institute of Oceanography, University of Georgia, Savannah, GA, 31411, USA.
 [3] State Key Laboratory of Estuarine and Coastal Research, East China Normal University, Shanghai, 200241, China

However, one sample of PE microplastics released organics or co-leachates that inhibited microbial growth. Thus, although sunlight may remove plastics from the ocean's surface, leachates formed during plastic photo-degradation may have mixed impacts on ocean microbes and the food webs they support.

1. Introduction

Over 5 trillion plastic items, dominated by < 5 mm microplastics (Eriksen et al., 2014), are afloat at sea and are affecting organisms from large mammals to the bacteria at the base of the ocean food web (Law, 2017). The potential impact of plastics on ocean life is increasing as plastic accumulates at the ocean's surface with large "garbage patches" forming in the subtropical gyres (Eriksen et al., 2014; Cozar et al., 2014; Sebille et al., 2015; Lebreton et al., 2018). Despite the accumulation of plastics at sea, only ˜1% of estimated annual inputs to the oceans are found afloat at the sea surface (Eriksen et al., 2014; Law, 2017; Cozar et al., 2014; Sebille et al., 2015; Law et al., 2010). Removal mechanisms for buoyant macro and microplastics have been proposed, including consumption by marine life (Law, 2017; Sebille et al., 2015; Davison and Asch, 2011), biofouling and/or aggregation with organic detritus leading to sinking (Kaiser et al., 2017; Kooi et al., 2017; Porter et al., 2018; Zhao et al., 2017; Zhao et al., 2018), deposition in under-sampled remote locations (Lavers and Bond, 2017), under-sampling of mega-plastics (Lavers and Bond, 2017) and degradation to small particles or solutes that will pass the 335 μm tow nets used to sample the smallest plastics at sea (Law, 2017; Poulain et al., 2018). However, few of these processes have been quantitatively assessed (Law, 2017).

Away from the ocean, the degradation of plastics has been studied for decades. Processes include biotic (mainly microbial), thermal, and photodegradation (Hakkarainen and Albertsson, 2004). Bio- and thermal-degradation proceed slowly at the low to moderate temperatures experienced at the earth's surface, making ultraviolet light exposure the most important factor in determining the rate of plastic degradation (Hakkarainen and Albertsson, 2004). Photodegradation reduces polymer molecular weight through scission reactions, forms novel non-oligomer structures through cross-linking reactions, oxidizes the polymer hydrocarbons, and produces gaseous products such as CO and CO_2 and a suite of low molecular weight and oxidized products (Ranby and Lucki, 1980; Gewert et al., 2015), some of which can be utilized by microbes (Hakkarainen and Albertsson, 2004).

These earlier studies, conducted in non-marine settings, led to the hypothesis that sunlight-driven photoreactions should be an important sink of buoyant plastics at sea (Andrady, 2015). The potential for sunlight to photodegrade plastics at sea is clear when it is considered that oceanic plastics accumulate in the oceanic subtropical gyres (Eriksen et al., 2014; Cozar et al., 2014; Sebille et al., 2015) which receive about 55% of the ultraviolet sunlight reaching the earth's surface (Powers et al., 2017) and buoyant plastics > 1 mm in size should spend the vast majority of their time at the sea surface (Enders et al., 2015). However, direct, experimental evidence for the photochemical degradation of marine plastics remains rare.

In marine settings, it was recently reported that exposure of microplastics to environmentally relevant light can release oxidized low molecular weight compounds dominated by dicarboxylic acids (Gewert et al., 2018) and the greenhouse gases methane and ethylene (Royer et al., 2018). Exposure to ultraviolet light can also photo-fragment polystyrene microplastics into nanoplastics (30 nm to 2 μm) (Lambert and Wagner, 2016) producing plastic fragments small enough to escape detection as microplastics at sea (effective cutoff in fieldwork > 335 μm). Finally, a study reported that dissolved organic carbon (DOC) is released as a pulse when plastics are first added to seawater, but that this occurs at similar rates in both the dark and under sunlight (Romera-Castillo et al., 2018). DOC is quantified as the organic carbon that passes through a sub-micron filter (Dittmar, 2014). Therefore, although DOC from microplastics may include sub-2 μm nanoparticles as well as

truly dissolved compounds (Romera-Castillo et al., 2018), the production of DOC unambiguously represents a loss of plastics from the size classes accounted for in marine plastic budgets (*i.e.* > 335 μm).

Naturally occurring DOC is the main source of carbon to microbes at the base of marine food webs (Moran et al., 2016) and constitutes a major store of global carbon approximately as large as the atmospheric CO_2 pool (Dittmar, 2014). Romera-Castillo et al. showed that the DOC leached from plastics was also available for uptake by microbes, suggesting that the accumulation of plastics in the ocean gyres could impact carbon cycling and microbial ecology in these major global biomes (Romera-Castillo et al., 2018).

Romera-Castillo et al. studied the release of DOC from PE and PP (Romera-Castillo et al., 2018). In the current study, we added EPS to the types of postconsumer polymers studied and included a neustonic sample of plastic-fragments from the North Pacific Gyre. Furthermore, we irradiated our samples under simulated sunlight for approximately 2 months capturing the kinetics of plastic dissolution. The plastic polymers were chosen as they are prevalent in surface ocean samples (Lebreton et al., 2018; Erni-Cassola et al., 2019) and have densities lower than seawater (densities: seawater ˜1.05 g cm⁻³; PE 0.91–0.94 g cm⁻³; PP 0.83–0.85 g cm⁻³; EPS variable, but below 1 g cm⁻³) (Andrady, 2015). For these experiments, the loss of plastic mass and carbon was determined at the end of experiments, while DOC was monitored throughout providing a time-series of plastic photo-dissolution and accumulation as DOC. Optical microscopy, electron microscopy, and Fourier transform infrared (FT-IR) spectroscopy were used to assess the physical and chemical photodegradation of plastics. Finally, the proportion of leached DOC that was bioavailable and the impact of leached organics upon microbial growth were assessed during bioassays with natural marine bacteria.

2. Experimental

2.1. Seawater and general sample handling

All sample handling and experimental procedures followed trace clean oceanic protocols for DOC (Stubbins and Dittmar, 2012). All plasticware was cleaned by triple rinsing with ultrapure water (MilliQ), soaking overnight in ˜pH 2 water (4:1000, v:v, 6 N HCl:MilliQ), triple rinsing with MilliQ and then drying. Glassware and quartzware were cleaned as above and then ashed at 450 °C for 6 h to remove any trace organics. Seawater (salinity ˜35) was collected from ˜5 m in the South Atlantic Bight using Niskin bottles aboard the RV *Savannah* and gravity-filtered (0.2 μm; AcroPak™ 1500, PALL) directly from Niskin bottles into pre-cleaned 20 L high density PE carboys. In order to remove natural, photochemically active organics before adding plastics, seawater was transferred to 2 L ashed quartz flasks and placed under germicidal ultraviolet-C light until colored dissolved organic matter was undetectable using an Aqualog spectrofluorometer (HORIBA Scientific) and the DOC concentration was stable.

2.2. Plastic preparation

Plastic particles collected from the North Pacific Gyre were provided by Algalita Marine Research and Education and the 5 Gyres Institute. The real-world North Pacific Gyre sample contained plastic-fragments with an average size of 5.9 ± 3.1 mm (Fig. S1), including sub-5 mm microplastics and other small plastic fragments. Thus, we refer to this sample as containing plastic-fragments rather than using the more precise, operational term microplastics that refers specifically

to particles under 5 mm (Law, 2017). Plastic particles were sonicated in MilliQ water for 10 min and then soaked in 1% H_2O_2 for two hours, and then triple sonicated for 5 min in MilliQ water. Once clean, the plastics were air dried prior to further analysis and use in experiments.

Postconsumer plastics were PE (RejoiceTM shampoo bottle), PP (NIVEA® facial cleanser bottle) and EPS (disposable lunch box). Postconsumer plastics were cut into small pieces (3.04 ± 0.87 mm; Fig. S1B-D). In addition, a standard PE granule (PEstd) was purchased (diameter: 2 mm; Goodfellow, USA). Prior to further analysis and experiments, microplastics were cleaned by sonification in MilliQ water and dried.

The surface area and volume of each sample type was estimated as described in the Supplementary Methods. Surface area to volume ratios (SA:V) were for each sample type were then calculated (Table1).

Density of each postconsumer microplastics was assessed by the addition of microplastics to MilliQ water and then either calcium or ethanol was added to adjust the solution density until the microplastics maintained in a position of neutral buoyancy for 20 min (Morét-Ferguson et al., 2010). 1 mL of the resultant solution was weighed to determine solution density. Measured densities are reported in Table S1. The density of EPS could not be determined via this method due to the presence of embedded air pockets. Therefore, data (0.01–0.05 g cm^{-3}) from the manufacturer are reported (https://insulationcorp.com/eps/).

2.3. Irradiations

All plastics were cleaned by sonification in MilliQ water and dried prior to experiments to simulate prior exposure to water as expected for plastics found at sea. Four hundred and eighty cleaned pieces of each polymer type were randomly selected, weighed (XP26 DeltaRange, Mettler Toledo, readability is 0.01 mg), and divided into two groups (240 particles per group). For the North Pacific Gyre sample, plastic-fragments were evenly separated into two groups based on mass (AB265 S/FACT, Mettler Toledo, readability is 0.01 mg). This yielded a total of twelve plastic aliquots: $2 \times$ PE, $2 \times$ PE standard, $2 \times$ EPS, $2 \times$ PP and $2 \times$ North Pacific Gyre. Prior to irradiation these aliquots were rinsed three times with MilliQ, three times with seawater and then transferred into the 2 L ashed and ultraviolet-C sterilized spherical quartz irradiation flasks with 1 L of pre-photobleached seawater (two flasks for each plastic type = 10 flasks). Two control flasks were filled with pre-photobleached seawater, without plastics resulting in a total of 12 flasks. Half of the flasks (*i.e.* one of each treatment) were wrapped in heavy duty aluminum foil to provide dark controls. All flasks were then placed inside a solar simulator.

Irradiations were conducted in a solar simulator system equipped with 12 UVA-340 bulbs (Q-Panel) which provides light with a spectral shape and flux approximating natural sunlight irradiance from 295 to 365 nm (Stubbins et al., 2012). This wavelength range is responsible for the majority of environmental polymer photochemical reactions (Andrady et al., 1996; Zhang et al., 1996; Stubbins et al., 2017). The integrated irradiance (14 ± 0.7 W m^{-2}) in the solar simulator was quantified using a spectroradiometer (OL 756, Optronic Laboratories) fitted with a quartz fiber optic cable and 2-inch diameter integrating sphere which was calibrated with a National Institute of Standards and Technology (NIST) standard lamp (OL752-10 irradiance standard) (Stubbins et al., 2017). Twenty four hours irradiation under these conditions approximates one solar day of photochemical exposure in the subtropical ocean gyre surface waters (Powers et al., 2017) where microplastics accumulate. A side mounted fan maintained temperatures between 25 °C and 30 °C. The flasks were repositioned daily to average out potential spatial variation in the light flux under the solar simulator. Throughout the seawater incubations DOC was monitored providing a time-series of DOC release and accumulation. In detail, liquid samples were drawn from the flasks using ashed glass Pasteur pipettes. Duplicate DOC samples (~10 mL aliquots) per time point were collected into pre-combusted 24 mL glass vials at 0 d, 2 d, 5 d, 10 d, 14 d, 22 d, 35 d, 49 d, 68 d for the North Pacific Gyre sample and 0 d, 0.5 d, 1 d, 3 d, 6 d, 10 d, 15 d, 22 d, 35 d, 54 d for postconsumer and standard plastic samples. Samples for bacteria counts (1 mL aliquots in sterile Nalgene cryovials) were collected at 0 d, 1 d, 15 d and 54 d for postconsumer and standard microplastics and at 0 d, 2 d, 5 d, 10 d, 14 d, 22 d, 35 d, 49 d, 68 d for the North Pacific Gyre sample, fixed with 0.1% glutaraldehyde, and frozen at -80 °C until analysis. The remaining volume of each sample for the next time point irradiation was determined based on weight. Plastics were recovered from the flasks by filtering through 0.22 μm filters (GVWP04700, Millipore). After 54 days, fragments were dried, weighed and further analyzed for carbon content, and via optical and electron microscopy, and Fourier transform infrared (FTIR) spectroscopy.

2.4. Carbon content of plastics

The mass of carbon as a percentage of total plastic mass was determined using an elemental analyzer (Flash 2000, Thermo Scientific). For the postconsumer and standard plastics, plastic was cut into small pieces and then cleaned and dried at 60 °C overnight. Duplicates for each plastic type were weighed (0.8 to 3 mg) on a microbalance (M2P, Sartorius) before being placed in tin cups (Costech) for combustion and carbon quantification in the elemental analyzer. 2,5-Bis (5-tert-butyl-

Table 1

Initial, final and loss of plastic mass, carbon content and carbon mass as well as dissolved organic carbon (DOC) production during the photochemical irradiation of postconsumer expanded polystyrene (EPS), polypropylene (PP) and polyethylene (PE), and standard PE (PE$_{std}$), and for North Pacific Gyre plastic during the irradiation (NPG$_{light}$) as well as during dark incubations (NPG$_{dark}$). Data for dark incubations of the postconsumer and standard microplastics are shown in Table S2.

		EPS	PP	PE	PE$_{std}$	NPG	NPG$_{dark}$
Initial	Surface area : volume ratio (cm^{-1})	12	44	36	33	22	22
	Plastic mass (mg-plastic)	47	334	298	2256	1887	1881
	Plastic carbon content (% C)	90 ± 1	86.6 ± 0.5	86 ± 1	86.3 ± 0.3	83 ± 1	83 ± 1
	Plastic carbon (mg-C)	42 ± 1	289 ± 2	256 ± 3	1947 ± 6	1560 ± 30	1560 ± 30
Final	Plastic mass (mg-plastic)	44	322	297	2249	1762	1875
	Plastic carbon content (% C)	88 ± 1	84.5 ± 0.6	87.1 ± 0.9	85.4 ± 0.2	n.d.	n.d
	Plastic carbon (mg-C)	38.6 ± 0.5	273 ± 2	259 ± 3	1920 ± 4	1460 ± 30	1550 ± 30
Loss of plastic	Plastic mass loss (mg-plastic)	2.5	11.5	1.3	6.8	125	6.0
	Plastic mass loss (%)	5.40	3.45	0.45	0.30	6.62	0.32
	Plastic carbon loss (mg-C)	3.5 ± 0.5	17 ± 2	-3 ± 3	26 ± 6	100 ± 27	0 ± 30
	Plastic carbon loss (%)	8 ± 1	5.8 ± 0.7	-1 ± 1	1.4 ± 0.3	7 ± 2	0 ± 2
DOC production	DOC production (mg-C)	2.87 ± 0.04	11.32 ± 0.09	0.28 ± 0.06	9.3 ± 0.1	25.3 ± 0.3	2.16 ± 0.05
	DOC production (% of initial plastic C)	6.8 ± 0.1	3.91 ± 0.03	0.11 ± 0.02	0.48 ± 0.01	1.62 ± 0.02	0.14 ± 0.00
	Loss of plastic C accounted for as DOC (%)	80 ± 20	70 ± 10	0 ± 120	40 ± 20	20 ± 30	0 ± 500

Notes: n.d. not determined. Errors reported as $\pm$ standard deviations to 1 significant figure. Where no errors are reported, standard deviations were less than 0.1% of the reported value.

benzoxazol-2-yl) thiophene (BBOT, CAS Number: 031047, Costech) was used as a standard material (Sharp, 1974). Due to the heterogeneity of the microplastic samples from the North Pacific Gyre, microplastic pieces were ground into a powder. Six aliquots of this powder were analyzed as above. Postconsumer and standard microplastics were analyzed as above before and after irradiation. North Pacific Gyre samples were only analyzed prior to irradiation.

2.5. Optical and scanning electron microscopy

Optical photographs of the microplastics before and after irradiation were collected using a Leica M165 FC microscope. The surface topography of the polymers before and after irradiation was characterized via scanning electron microscopy (SEM, Hitachi S-4800, Japan). For SEM, plastic samples were coated with a light conductive gold prior to analysis to prevent sample charging (Corcoran et al., 2009).

2.6. Fourier transform infrared (FTIR) spectroscopy

In order to assess the chemistries of plastic-fragments within the North Pacific Gyre sample, 51 cleaned plastic particles (0.49 g, 5.9 ± 3.1 mm, Figs. 1 and S1A) were selected randomly for morphological characterization and polymer identification via attenuated total reflection (ATR) μ-FTIR (Bruker Lumos). Duplicate μ-FTIR spectra (600 to 4000 cm^{-1}; resolution 4 cm^{-1}) were acquired for different locations on each plastic-fragment and compared against a library of reference spectra (BioRad-KnowItAll Informatics System, Thermo Fisher Scientific Inc.). After identification, the mass of each plastic type was weighed.

To assess polymer photo-oxidation during experiments, a Nicolet iS5 FT-IR Spectrometer (Thermo Fisher Scientific Inc.) was used to determine the carbonyl content of the postconsumer and plastic standard samples at time zero, after 54 days of sterile dark incubation, and after 54 days of sterile irradiation. Triplicate spectra were recorded at 32 scans and 4 cm^{-1} resolution in the range of 400–4000 cm^{-1} using the ATR mode with the same pressure. All the spectra were corrected by subtracting the average value of 3900–4000 cm^{-1}. Carbonyl content was determined as the maximum value from 1700–1800 cm^{-1} of the corrected spectra (Rajakumar et al., 2009).

2.7. Dissolved organic carbon (DOC)

Samples for DOC analysis were acidified to pH < 2 using HCl (p.a.)

before analysis using a Shimadzu TOC-VCPH total organic carbon analyzer (Stubbins and Dittmar, 2012). Certified DOC standards (low carbon seawater, LSW and deep seawater reference material, DSR) from the Consensus Reference Materials (CRM, University of Miami) were measured to confirm precision and accuracy. Measured DSR values were consistent with the consensus value (0.49-0.53 mg L^{-1}, http://yyy.rsmas.miami.edu/groups/biogeochem/Table1.htm) with a standard deviation < 5%. Routine minimum DOC detection limits using the above configuration are 0.034 ± 0.0036 mg L^{-1} and standard errors are typically 1.7 ± 0.5% of the DOC concentration (Stubbins and Dittmar, 2012).

Plastic carbon mass normalized DOC accumulation was calculated following Eq. (1).

$$P_{DOC} = \frac{\sum_{i=1}^{n} (V_i C_i - V_{i-1} C_{i-1})}{M_C initial} \tag{1}$$

Where, P_{DOC} is the accumulation of DOC produced during the photodissolution of microplastics; n is the total number of samplings; i is each time point; V and C are the sample volume and concentration at each time point, respectively, and; $M_{C\ initial}$ denoted the total plastic carbon mass (g) of plastic particles at the start of each experiment. Measurement uncertainties were propagated to calculate final errors (Taylor, 1997).

2.8. Bioassays and flow cytometry

The biolability of DOC released during photodegradation of the postconsumer and standard plastics was determined via dark incubation bioassays following previous methods (Spencer et al., 2015, 2014; Holmes et al., 2008). In brief, the 0.2 μm filtered plastic DOC samples collected after irradiation were separated into 24 mL pre-combusted glass vials (18 mL sample per vial). Coastal seawater from Skidaway dock (31.9885 °N, 81.0212 °W, salinity = 27.7) was first filtered through 1 μm syringe filter (Paradisc™) to remove large particles and grazers but leave most microbes in the filtrate. Each vial was inoculated with 180 μL of the filtrate. Nutrient solution (0.5 g L^{-1} $NaNO_3$ and 0.05 g L^{-1} K_2HPO_4) was supplemented depending on the sample carbon concentration to make sure the carbon:nitrogen:phosphorus ratio was above the Redfield ratio (*i.e.* C:N:P > 106:16:1) (Redfield, 1934), preventing nitrogen and phosphorous limitation of microbial carbon utilization. Samples were incubated in the dark on a shaker table (45 rpm) at room temperature (~20 °C). After 1 d, 3 d, 7 d, 15 d, 28 d, 62 d and 92 d samples were sacrificed. Aliquots were taken for bacteria
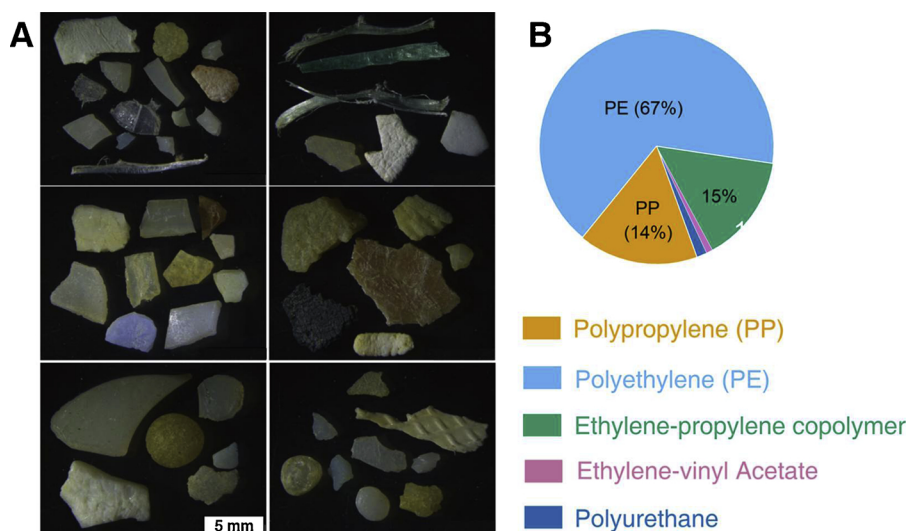

Fig. 1. Microscopic photographs (A) and polymer chemistry composition (B) of 51 microplastic particles from the North Pacific Gyre. The polymer type for each of the 51 particles was determined via micro-Fourier transform infrared spectroscopy.

enumeration via flow cytometry and DOC analysis (Section 2.7). DOC losses in the control, irradiated seawater sample without plastics were subtracted from the plastic DOC losses.

The decrease in DOC during incubations was described by a single, three parameter exponential decay model:

$$C(t) = C_\infty + z_0^{-kt} \qquad (2)$$

Where, $C(t)$ = the DOC concentration (mg L^{-1}) analysed at time (t); C_∞ = an adjustable parameter that represents the non-bioreactive (*i.e.* biorefractory) DOC component (*i.e.* the DOC concentration that is predicted to survive at time equals infinity); z_0 = an adjustable component that represents the concentration of bioreactive DOC at time = 0; k = the rate of decay and t = the time (days).

Flow cytometry data were collected during the bioassays to monitor microbial growth on photoproduced DOC. Liquid samples for bacteria counts (~1 mL) were preserved with 0.1% glutaraldehyde and stored at −80 °C until analysis on a Guava flow cytometer (Millipore, Billerica MA), equipped with a blue laser (excitation at 488 nm), emission detectors at 525, 575 and 695 nm, and side and forward scatter detectors. The instrument was calibrated with fluorescent beads (Millipore) according to the manufacturer's instructions. Samples were vortexed, and 300 μL sample aliquots were screened through a clean 50 μm mesh and 200 μL of the screened sample were further pipetted into a 96-well plate and dyed using 2 μL SYBR Green I (1 x, final concentration, Invitogen) for 30 min in the dark. Filtered seawater and 0.2 μm-filtered samples were run as blanks. Data were acquired and analyzed using the GuavaSoft InCyte software (v. 3.1.1). Cell counts were determined by plots of green (525 nm) versus side scatter fluorescence (Gasol and Del Giorgio, 2000).

In addition, and following the method detailed above, flow cytometry was used to assess whether the original photo-irradiations of microplastics were sterile. These experiments were designed to be sterile in order to allow the assessment of abiotic light and dark microplastic degradation without any bacteria present (*i.e.* to assess the direct photodegradation of plastics). Periodic bacterial abundance measurements via flow cytometry confirmed samples were sterile. Counts detected in flow cytometry blanks reflect instrument background noise (maximum: 559 counts) and counts in microplastic samples were below the instrument noise level (maximum: 402 counts, Fig. S2). Based upon this data, we conclude that samples were sterile throughout the microplastic photodegradation experiments. Clearly, the bioassay experiments were not sterile neither in practice nor by design.

3. Results

3.1. Initial characterization of buoyant North Pacific gyre plastic-fragments

Based upon FT-IR data, approximately 67% of the fragments in the real-world North Pacific Gyre sample were polyethylene (PE), 16% were polypropylene (PP), and 15% were ethylene-propylene copolymers, with minor contributions from polyurethane (1.4%) and ethylene vinyl acetate copolymer (0.86%; Fig. 1). The prevalence of PE with significant contributions of PP is consistent with previous data for microplastic chemistries in the North Pacific Gyre (Lebreton et al., 2018) and other open ocean locations (Law et al., 2010; Enders et al., 2015; Erni-Cassola et al., 2019).

3.2. Photochemical changes in plastic properties

Flow cytometry revealed all dark and light incubations of plastics to be sterile throughout (Fig. S2). All plastics remained afloat during the seawater experiments. No chemical or optical changes were observed for plastics incubated in the dark (Figs. 2 and 3). Following irradiation, EPS yellowed (Fig. 2A and B) and PP and PE became cloudy (Fig. 2E,F,I and J), but no visible change was observed for PE$_{std}$. Photo-fragmentation was evidenced by the presence of extensive cracks, fractures, flakes and pits in scanning electron microscopic (SEM) images of the
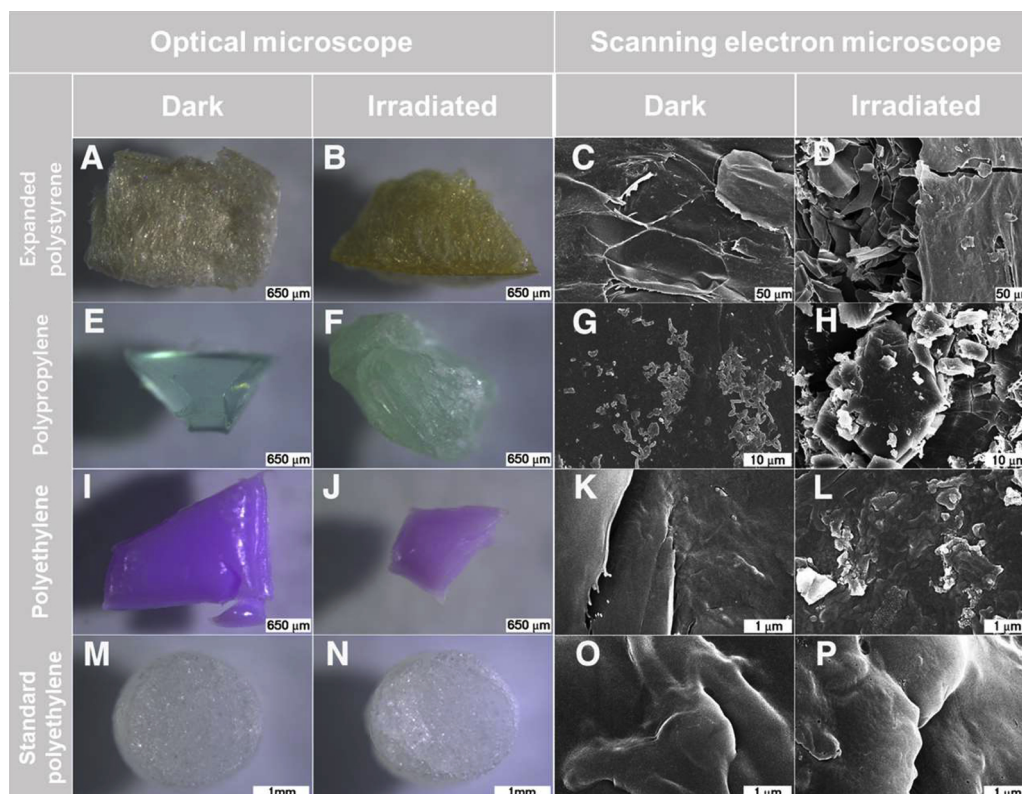

Fig. 2. Optical and scanning electron microscopic photographs of dark and irradiated microplastic samples.
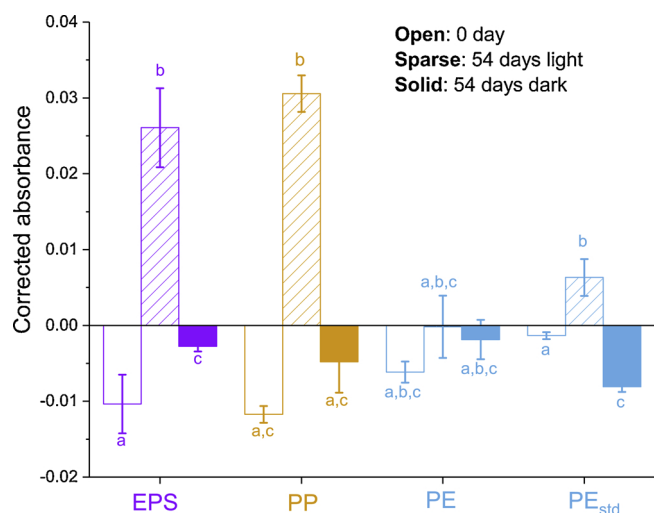
Fig. 3. Changes in polymer carbonyl absorbance duri ng irradiation. **EPS:** postconsumer expanded polystyrene. **PP:** postconsumer polypropylene. **PE:** postconsumer polyethylene. **PE_std:** standard PE. The raw absorbance is corrected by subtracting the average value of 3900–4000 cm^{-1}. Bars of each polymer sharing the same letter are not significantly different (p > 0.05, T-Test).

photo-irradiated EPS, PP and PE_std samples (Fig. 2C,D,G,H,O and P), but not in the SEM images of PE samples (Fig. 2K and L). Polymer carbonyl content was constant in the dark and increased during irradiations of EPS, PP and PE_std with the greatest enrichment observed for EPS followed by PP and PE_std (Fig. 3). No increase in carbonyl content was observed for PE (Fig. 3).

3.3. Loss of plastic mass and carbon

After 54 days floating on sterile seawater in the dark, the mass of microplastics and mass of microplastic carbon recoverable from the incubations of EPS, PP, PE and PE_std was within error of initial values (Table S2). Under simulated sunlight, the PE sample was reduced in mass, but not reduced in carbon or in its percentage carbon by mass (Table 1). The EPS, PP and PE_std samples all lost plastic and carbon mass (Table 1). The percentage carbon by mass of each of these microplastics also decreased, suggesting the incorporation of other

elements (*e.g.* oxygen through photo-oxidation) into the remaining polymers.

In the dark, the North Pacific Gyre sample reduced in mass by 6.0 mg-plastic (0.32%) after 68 days, but the loss of plastic carbon was not different from zero given the methods used (0 ± 30 mg-C or 0 ± 2%; Table 1). Under simulated sunlight, the North Pacific Gyre plastic-fragments reduced in mass by 125 mg-plastic (6.6%) and by 100 ± 30 mg-C (7 ± 2%; Table 1). The carbon content of the North Pacific Gyre samples was not measured post-irradiation. Thus, these estimates of carbon loss are based upon mass loss and the percentage carbon by mass of the initial plastic-fragments.

3.4. DOC accumulation

DOC concentrations in control samples without plastics remained constant in the light (1.01 ± 0.01 mg-C L^{-1}) and dark (1.00 ± 0.03 mg-C L^{-1}). The stability of background DOC indicated that any changes in DOC production in experiments with plastics could be attributed to the plastics added. For the North Pacific Gyre experiment, DOC accumulated ~10 times faster under simulated sunlight (linear leaching rate: 0.235 ± 0.003 mg DOC g-C^{-1}d^{-1}) than in the dark (0.024 ± 0.003 mg DOC g-C^{-1}d^{-1}; Fig. 4A, Table S3). None of the postconsumer or standard plastic samples released DOC in the dark, whereas DOC accumulated during all irradiations (Fig. 4B–D, Table S3). After 54-day irradiations, the seawater sample containing EPS accumulated the greatest amount of DOC (68.2 ± 0.9 mg DOC g-C^{-1}), followed by PP (39.1 ± 0.3 mg DOC g-C^{-1}), PE_std (4.8 ± 0.1 mg DOC g-C^{-1}), and PE (1.1 ± 0.2 mg DOC g-C^{-1}; Fig. 4B–D). Based upon carbon, these values equate to the photo-dissolution of 6.8 ± 0.1% of EPS, 3.91 ± 0.03% of PP, 0.48 ± 0.01% of PE_std, and 0.11 ± 0.02% of PE within 54 days (Table 1). Comparison of DOC production to the mass of plastic carbon lost during the irradiations indicated that 80 ± 20% of EPS carbon, 70 ± 10% of PP carbon, -0 ± 120% of PE carbon, 40 ± 20% of PE_std carbon, and 20 ± 30% of North Pacific Gyre plastic carbon lost during the irradiations ended up as DOC (Table 1). Finally, DOC leaching from PE_std, PP, and EPS accelerated over the 54 days of irradiations (Fig. 4), whereas the North Pacific Gyre sample and post-consumer PE photo-leached DOC at a constant rate (Fig. 4A and D).
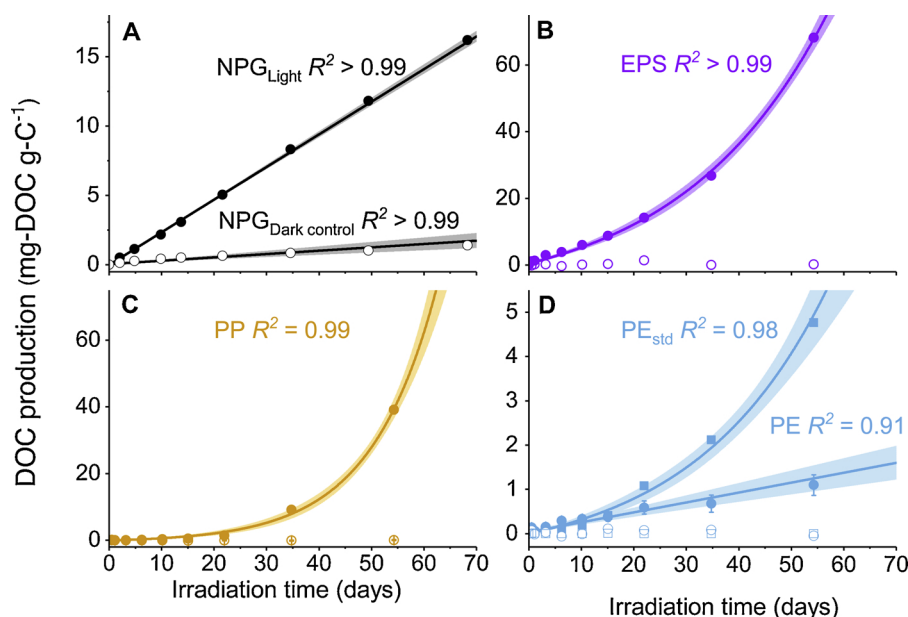

Fig. 4. Initial plastic carbon mass normalized dissolved organic carbon (DOC) accumulation kinetics during irradiations of different plastic samples. A) North Pacific Gyre (NPG); B) postconsumer expanded polystyrene (EPS); C) postconsumer polypropylene (PP), and; D) post-consumer polyethylene (PE; circle) and standard PE (PE_std; square). Filled symbols represent irradiated samples. Open symbols represent dark controls. The equations describing DOC accumulation are shown in Table S3.

3.5. Microbial utilization of and response to photo-leached plastic DOC

DOC concentrations in all bioassays, except the PE_{std} bioassay, decreased following 1st order decay kinetics with fits having R^2 above 0.9 and p below 0.001 (Figs. 5A, S3, Table S4). The photo-irradiated seawater control contained 0.41 ± 0.03 mg L^{-1} of biolabile DOC. EPS DOC was the most biolabile, with $76 \pm 8\%$ DOC lost, followed by PP DOC ($59 \pm 8\%$), PE DOC ($46 \pm 8\%$) and PE_{std} DOC ($22 \pm 4\%$) (Fig. 5A). For the seawater control without any plastic-derived DOC and for seawater containing EPS DOC and PP DOC, bacteria bloomed and then decreased by day-92 of the bioincubation (Fig. 5B). For seawater containing PE DOC, bacteria numbers increased and then remained stable until day-62 with no data for day 92 (Fig. 5B). Bacterial growth was inhibited in all the replicates containing PE_{std} DOC (single, independent replicates were sacrificed at 8 time points with duplicates at 7 days, totaling 9 independent replicate incubations).

4. Discussion

4.1. Stability of microplastics in the dark

Floating on sterile seawater in the dark, postconsumer and standard polymers did not lose measurable carbon, leach measurable DOC (Fig. 4, Table S3) or show any visible or chemical signs of degradation (Fig. 3). These results indicate that our samples of EPS, PE and PP were stable in the absence of light under sterile conditions. Although plastic-fragments from the North Pacific Gyre did leach DOC in the dark, rates were 10 times lower than in the light (Fig. 4A, Table S3). Prior to irradiation in the laboratory, PE and PP plastic-fragments from the North Pacific Gyre exhibited micro-cracks (Fig. S4C and D) and carbonyl absorbance (Fig. S4B) consistent with oxidation at sea (Brandon et al., 2016). The photo-oxidation of plastics can enhance their subsequent leaching of organics (Eyheraguibel et al., 2018). Therefore, the slow leaching of DOC from North Pacific Gyre plastic-fragments in the dark could be related to the pre-exposure of these plastics to photo-oxidation or other forms of weathering at sea. Linear extrapolation of the rate of plastic mass loss in the dark (Table 1), indicated that 100% of the North Pacific Gyre plastic-fragments in our sample would be lost within 58 years (Table 2) with ~44% of the microplastic carbon ending up as DOC (Table 1).

4.2. Photo-dissolution and degradation of microplastics under simulated sunlight

Simulated sunlight degraded all plastics studied leading to fragmentation observed via scanning electron microscopy (Fig. 2), oxidation observed as an increase in carbonyl-content via FT-IR (Fig. 3), and dissolution, indicated by the accumulation of DOC (Fig. 4, Table S3). In the light, North Pacific Gyre plastic-fragments released DOC at a constant rate 10 times greater than in the dark (Fig. 4A) demonstrating that

Table 2

Lifetimes (*i.e.* time to lose 100% of microplastic mass or carbon) during the photochemical irradiation of postconsumer expanded polystyrene (EPS), polypropylene (PP) and polyethylene (PE), and standard PE (PE_{std}), and, for North Pacific Gyre plastic, during the irradiation (NPG_{light}) as well as during dark incubations (NPG_{dark}).

EPS^1	PP^1	PE^2	PE_{std}^1	NPG_{light}^2	NPG_{dark}^2
0.3-2.7 years	0.3-4.3 years	33 years	0.5-49 years	2.8 years	58 years

Notes: [1]maximum lifetime based upon linear extrapolation of plastic mass loss and minimum based upon the exponential increase in DOC accumulation rate observed for these plastic. [2]based upon linear extrapolation of plastic mass loss only.

this natural sample of mixed polymer chemistry was susceptible to photochemical degradation. The rates and kinetics of DOC production from the different plastics varied under the same irradiation conditions (Fig. 4). As photochemistry requires the absorbance of light, the surface area to volume ratio (SA:V) of the plastics could be an important factor in determining degradation rates. However, SA:V did not explain the trends in reaction rates. For instance, the EPS sample had the lowest SA:V but was the most photoreactive, while the PP, PE and PEstd samples all had similar SA:V ratios but exhibited wide variations in their photoreactivities (Table 1). Instead of SA:V, it is likely that plastic chemistry modulated the efficiency of plastics photodegradation. Photoreactions are initiated when light is absorbed producing free radicals that then attack and oxidize plastics (Gewert et al., 2015). The susceptibility of a chemical to direct photodegradation at the Earth's surface is determined by its ability to absorb sunlight, particularly at the higher energy ultraviolet wavelengths of the solar spectrum (~280 to 400 nm) and absorbance of light is in turn determined by the presence of conjugated chromophoric functional groups in a compound (Gewert et al., 2015). For instance, the aromatic chromophores that give natural DOC its color are the main absorbers of ultraviolet light in natural waters (Kitidis et al., 2006). As they absorb sunlight these dissolved aromatic compounds are rapidly and preferentially photodegraded in the surface ocean (Stubbins et al., 2012; Mopper et al., 2015). Of the plastics studied, only EPS contains chromophoric aromatic functional groups (Gewert et al., 2015). Thus, the presence of aromatic, sunlight absorbing structures in EPS that can directly initiate photoreactions is the likely explanation for the enhanced photodegradability of EPS microplastics compared to the other plastics studied (Fig. 4).

PP and PE do not contain conjugated chromophoric groups (Gewert et al., 2015). Consequently, completely pure PP and PE should neither absorb sunlight nor be photoreactive. However, the photoreactivity of PP and PE in non-ocean settings is well documented and believed to be due to the presence of intra-polymer chromophoric impurities or structural abnormalities (Gewert et al., 2015). Such impurities or abnormalities may explain the photoreactivity of the non-aromatic PP and PE microplastics irradiated here, at least at the start of the irradiations.
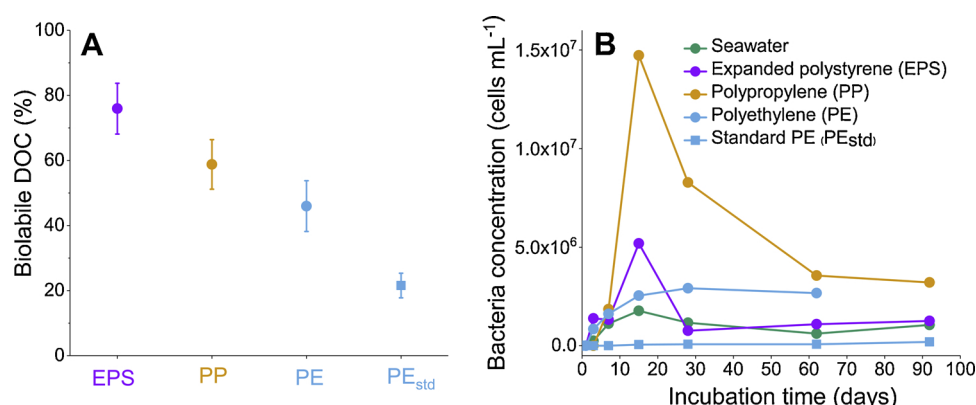

Fig. 5. Bacterial dissolved organic carbon (DOC) utilization and growth during 92-day incubations of marine bacteria with DOC derived from the photo-dissolution of microplastics. A) DOC utilization expressed as percent biolability (*i.e.* percentage of the original DOC removed by bacteria); B) bacterial growth curves for each incubation.

Differences in the levels of any impurities or abnormalities (*e.g.* oxidized functional groups) may also have caused the differences in photoreactivity of the PE and PE$_{std}$ samples.

Photoreaction rates in natural waters usually decrease exponentially as the most reactive reactants are removed with increasing irradiation time (Stubbins et al., 2012; Mopper et al., 2015). However, DOC photoleaching from PE$_{std}$, PP, and EPS accelerated over the course of the 54-day irradiations (Fig. 4B–D). This acceleration in plastic photodegradation with continuing irradiation has been observed in weathering tests as an acceleration in the rate of polymer oxidation (Tidjani, 1997). For continuous pieces of polymer, this acceleration is attributed to the accumulation of oxygen-containing moieties, particularly carbonyl and hydroperoxide, which can drive the sensitization and initiation of plastic photo-oxidation(Gewert et al., 2015; Geuskens and David, 1979; Carlsson et al., 1976). The photo-induced fragmentation observed for microplastics (Lambert and Wagner, 2016) could also accelerate photoreactions by increasing the surface area available to absorb sunlight. During our irradiations, polymer photo-oxidation (*i.e.* increase in carbonyl content; Fig. 3) and photo-fragmentation (Fig. 2) occurred. Photo-oxidation and fragmentation were most apparent for EPS and PP and may have contributed to the acceleration in DOC release from these polymers. By contrast, fragmentation and oxidation were less apparent for the more photo-stable PE samples (Figs. 2 and 3).

A previous study reported rapid initial DOC leaching from postconsumer PE and PP followed by slow leaching over the subsequent 30 days with no difference in DOC production in the dark or light (Romera-Castillo et al., 2018). By contrast, for postconsumer and standard polymers, we observed no DOC release in the dark and either an accelerating or constant rate of DOC release in the light (Fig. 4). The difference between this earlier study and our results may stem from differing experimental designs. The previous study quantified DOC leaching from freshly prepared, unrinsed microplastics to simulate the initial pulse of DOC leached when plastics enter natural waters (Romera-Castillo et al., 2018); whereas we pre-rinsed microplastics prior to leaching to simulate the potential for sustained release of DOC from plastics in the ocean. Taken together, these results suggest an initial pulse of DOC occurs as plastics enter natural waters, with little subsequent release of DOC in the dark, but increasingly efficient DOC release in the light. The finding that plastics are much more efficiently removed from the ocean surface under sunlight than in the dark is reported here for the first time and discussed in greater detail below.

4.3. Potential for sunlight to remove microplastics at the sea surface

There are many uncertainties that reduce the accuracy of estimates for sunlight-driven photochemical reaction rates at sea (Mopper et al., 2015). However, it is informative to estimate the potential for sunlight to remove microplastics from the ocean. During our irradiations, approximately 5.4% of the mass of EPS, 3.5% of PP, 0.5% of PE and 0.3% of PE$_{std}$ microplastics were lost within 54 days with the North Pacific Gyre plastic-fragments decreasing in mass by ~6.6% over 68 days (Table 1). Linear extrapolation of these loss rates provided estimates of the time taken to remove 100% of each plastic type under our experimental conditions (Table 2). EPS (2.7 years) and the North Pacific Gyre (2.8 years) samples had the shortest lifetimes, followed by PP (4.3 years), PE (33 years), and PE$_{std}$ (49 years). Carbon content provides a more accurate measure of the surviving microplastic hydrocarbon polymer than mass alone and the carbon content of the most photoreactive plastic decreased during the irradiations (Table 1). Thus, carbon-based estimates for the lifetimes for these microplastics are reduced to 1.8 ± 0.3 years for EPS, 2.6 ± 0.3 years for PP, and 11 ± 2 years for PE$_{std}$.

The above calculations for the persistence of plastics in sunlight rely upon linear extrapolations. However, our time series data for DOC accumulation indicate that EPS, PP and PE$_{std}$ photo-dissolution accelerated during the irradiations (Fig. 4B–D). Thus, for these

microplastics, we also estimated how many years of sunlight would be required to convert 100% of microplastic carbon to DOC using the exponential fits from our experimental DOC accumulation data (Table S3). These estimates suggest 100% of EPS, PP and PE$_{std}$ microplastics could be converted to DOC within 0.3, 0.3 and 0.5 years, respectively (Table 2). These estimates are only for losses to DOC, which account for 35 to 82% of the photochemical plastic loss for these samples (Table 1). In this sense, these estimates are conservative. However, due to the incorporation of acceleration, these estimates are approximately an order of magnitude faster than the linear model estimates for the same microplastics (see range of estimates for these plastics in Table 2).

The above considerations pertain to the lifetime of plastic in our experiments. In the laboratory, plastic remained afloat throughout the seawater irradiations, indicating photodegradation did not increase plastic density sufficiently for them to leave the seawater surface. In the open ocean, modeling studies indicate that fragments of buoyant PP and PE with sizes greater than 1 mm also remain afloat at the ocean surface (Enders et al., 2015). Twenty-four hours under our solar simulator equaled ~1 solar day of sunlight in the subtropical surface waters in which microplastics accumulate (Stubbins et al., 2012). Therefore, our irradiation conditions and resultant rates were presumed to be similar to those in the surface ocean (*i.e.* 1 day in the lab = 1 solar day in the ocean). Based upon our results under these conditions, sunlight has the potential to degrade EPS, PP, some forms of PE microplastics, and the plastic-fragments within the composite North Pacific Gyre sample to the sub 0.2 μm size class within months to years (Table 2). Microplastics are usually defined as having a lower size cutoff of 1 mm (1000 μm) (Law, 2017). Thus, sunlight appears to be important for reducing plastics to sizes below those captured by oceanic studies and explaining how > 98% of the plastics entering the oceans go missing each year (Law, 2017). However, further field, experimental and modeling work is required to improve estimates of the rates of photochemical degradation of plastics in the ocean.

The relative photodegradability of the polymers irradiated here are consistent with oceanic trends in polymer distributions. To accumulate in the subtropical gyres, microplastics of continental or coastal origin must first transit oceanic circulation pathways. For example, microplastics require an estimated 8 years to reach the North Pacific Gyre from Shanghai (31.2 °N, 122 °E) (Maximenko et al., 2012). During transit, photodegradation will presumably reduce the total amount and alter the chemistry of microplastics. EPS is prevalent in coastal waters (Lee et al., 2015; Sadri and Thompson, 2014; Sun et al., 2018), while scarce in the open ocean (Lebreton et al., 2018; Law et al., 2010); and PP decreased from 49% of microplastics in the California Current to 12% in the North Pacific Gyre, with PE being the most abundant microplastic in the gyre (86% of microplastics) (Brandon et al., 2016). The comparative photodegradability of these plastics may explain these trends. For instance, the scarcity of EPS and decline of PP abundance towards the gyres may be a product of these two polymers' high photodegradability, whereas the persistence and relative enrichment of PE in the gyres compared to coastal waters is consistent with PE's relative photo-stability. As for assessments of absolute rates of plastic photodegradation at sea, further work is also required to assess the relative photodegradability for more replicates of the polymers irradiated here (*i.e.* different formulations of EPS, PE and PP should be irradiated) and to assess the kinetics of plastic mass and carbon loss.

4.4. Biolability and impact of plastic-derived DOC upon marine microbes

Concentrations of EPS, PP and PE-derived DOC in the bio-incubation experiments decreased following 1st order decay kinetics (Fig. S3) as observed for natural DOC (Spencer et al., 2015; Bittar et al., 2015). Microbial removal and chemical alteration of intact, non-photo or thermally-oxidized plastics is slow to non-detectable in natural systems (Eyheraguibel et al., 2018). By contrast, the DOC produced from most microplastics in the current study was rapidly biodegraded (Figs. 5 and

S3). The photo-oxidation of plastics leads to the leaching of diverse, low molecular weight organics (Hakkarainen and Albertsson, 2004; Eyheraguibel et al., 2018). Of the soluble, low molecular weight organics identified in the DOC pool leached from photodegraded PE, 95% were utilized by a single strain of bacteria (Eyheraguibel et al., 2018). Thus, the photochemical conversion of plastics to highly biolabile low molecular weight compounds likely explains why photoproduced DOC from EPS, PP and PE in the current experiments was also highly biolabile. The percentage of biolabile EPS, PP and PE DOC (Fig. 5A) were comparable to some of the most biolabile forms of DOC from natural sources (*e.g.* phytoplankton cultures: 40% to 75% biolabile (Bittar et al., 2015) and permafrost thaw waters: ~50% biolabile (Spencer et al., 2015), indicating that photodegradation of these plastics yields DOC that will be rapidly utilized by microbes at the sea surface. The photochemical production of DOC from plastics is a modest flux compared to in situ, natural DOC cycling. However, the input of novel forms of organics to the ocean's surface could perturb microbial communities. For instance, a change in the water column distribution and chemical forms of labile DOC could alter community activity and composition (Carlson et al., 2002).

Although most of the DOC generated as plastics photodegraded was highly biolabile (> 40%), only 22% of PE_{std} DOC was biolabile. Like all the plastic-derived DOC here, the PE_{std} DOC leached and accumulated in continuous sunlight, suggesting it is photo-resistant. Thus, ~80% of PE_{std} DOC may be resistant to both light and microbes and could survive and even accumulate in the surface ocean. A potential reason for the low biolability of PE_{std} DOC is suggested by the flow cytometry data. For seawater, EPS, PP and PE DOC, bacteria numbers followed the bloom and bust dynamics generally observed in inoculated bottle experiments (Fig. 5B). However, bacteria did not grow in any of the replicates to which PE_{std} DOC was added. The lack of growth even when compared to the seawater control suggest that, instead of being bio-resistant, DOC or some co-leachate released from PE_{std} during photodegradation may be bio-inhibitory. Additives, incorporated into polymers to alter plastic stability and other properties, could be a source of these inhibitory co-leachates. The potential that plastics are releasing bio-inhibitory compounds during photodegradation in the ocean could impact microbial community productivity and structure, with unknown consequences for the biogeochemistry and ecology of the ocean. In the current study, one of four polymers had a negative effect on bacteria. Thus, further work is required to determine whether the release of bio-inhibitory compounds from photodegrading plastics is a common or rare phenomenon.

5. Conclusions

There remains a lot to learn concerning the mass, size, and chemical distributions of plastics in the oceans, as well as the processes that control the oceanic lifetimes and environmental impact of these contaminants of emerging concern. Our results provide novel insight regarding the removal mechanisms, and potential lifetimes of a select few microplastics. For the most photoreactive microplastics, such as EPS and PP, sunlight may rapidly remove these polymers from ocean waters. Other, less photodegradable microplastics such as PE, may take decades to centuries to degrade even if they remain at the sea surface. As these plastics dissolve at sea, they release biologically active organic compounds, measured as total DOC in the current study. These dissolved organics seem to be broadly biodegradable and a drop in the ocean compared to natural biolabile marine DOC. However, some of these organics or their co-leachates may inhibit microbial activity. Thus, future work is required to better understand the rates at which plastics degrade at sea, the mechanisms responsible, and the chemistries and impacts of the byproducts released during the interactions of plastic, light and life in our oceans.

Author contributions

All authors were involved in conceiving the study. L.Z., S.Z. and A.S. designed the experiments. L.Z. and S.Z. conducted the experiments. L.Z., S.Z. and T.B. analyzed the samples. L.Z., S.Z., T.B and A.S. analyzed the data. L.Z. and A.S. wrote the manuscript with significant assistance and comments from all the other authors. All authors approve the final version of the manuscript.

Data and materials availability

All data needed to evaluate the conclusions in the paper are present in the paper and/or the appendix.

Declaration of Competing Interest

The authors declare no competing financial interest.

Appendix A. Supplementary data

Supplementary material related to this article can be found, in the online version, at doi:https://doi.org/10.1016/j.jhazmat.2019.121065.

References

Eriksen, M., Lebreton, L.C.M., Carson, H.S., Thiel, M., Moore, C.J., Borerro, J.C., Galgani, F., Ryan, P.G., Reisser, J., 2014. Plastic pollution in the world's oceans: more than 5 trillion plastic pieces weighing over 250,000 tons afloat at sea. PLoS One 9, e111913.

Law, K.L., 2017. Plastics in the marine environment. Annu. Rev. Mar. Sci. 9, 205–229.

Cozar, A., Echevarria, F., Gonzalez-Gordillo, J.I., Irigoien, X., Ubeda, B., Hernandez-Leon, S., Palma, A.T., Navarro, S., Garcia-de-Lomas, J., Ruiz, A., Fernandez-de-Puelles, M.L., Duarte, C.M., 2014. Plastic debris in the open ocean. Proc. Natl. Acad. Sci. U.S.A. 111, 10239–10244.

Sebille, V.E., Wilcox, C., Lebreton, L., Maximenko, N., Hardesty, B.D., Franeker, V.J.A., Eriksen, M., Siegel, D., Galgani, F., Law, K.L., 2015. A global inventory of small floating plastic debris. Environ. Res. Lett. 10, 124006.

Lebreton, L., Slat, B., Ferrari, F., Sainte-Rose, B., Aitken, J., Marthouse, R., Hajbane, S., Cunsolo, S., Schwarz, A., Levivier, A., Noble, K., Debeljak, P., Maral, H., Schoeneich-Argent, R., Brambini, R., Reisser, J., 2018. Evidence that the great pacific garbage patch is rapidly accumulating plastic. Sci. Rep.-Uk 8, 4666.

Law, K.L., Moret-Ferguson, S., Maximenko, N.A., Proskurowski, G., Peacock, E.E., Hafner, J., Reddy, C.M., 2010. Plastic accumulation in the North Atlantic subtropical gyre. Science 329, 1185–1188.

Davison, P., Asch, R.G., 2011. Plastic ingestion by mesopelagic fishes in the North Pacific Subtropical Gyre. Mar. Ecol. Prog. Ser. 432, 173–180.

Kaiser, D., Kowalski, N., Waniek, J.J., 2017. Effects of biofouling on the sinking behavior of microplastics. Environ. Res. Lett. 12, 124003.

Kooi, M., Nes, E.H.V., Scheffer, M., Koelmans, A.A., 2017. Ups and downs in the ocean: effects of Biofouling on vertical transport of microplastics. Environ. Sci. Technol. 51, 7963–7971.

Porter, A., Lyons, B.P., Galloway, T.S., Lewis, C., 2018. Role of marine snows in microplastic fate and bioavailability. Environ. Sci. Technol. 52, 7111–7119.

Zhao, S.Y., Danley, M., Ward, J.E., Li, D., Mincer, T.J., 2017. An approach for extraction, characterization and quantitation of microplastic in natural marine snow using Raman microscopy. Anal. Methods-Uk 9, 1470–1478.

Zhao, S., Ward, J.E., Danley, M., Mincer, T.J., 2018. Field-based evidence for microplastic in marine aggregates and mussels: implications for trophic transfer. Environ. Sci.

Technol. 52, 11038–11048.

Lavers, J.L., Bond, A.L., 2017. Exceptional and rapid accumulation of anthropogenic debris on one of the world's most remote and pristine islands. Proc. Natl. Acad. Sci. U.S.A. 114, 6052–6055.

Poulain, M., Mercier, M.J., Brach, L., Martignac, M., Routaboul, C., Perez, E., Desjean, M.C., ter Halle, A., 2018. Small microplastics As a main contributor to plastic mass balance in the North Atlantic subtropical gyre. Environ. Sci. Technol. 53, 1157–1164.

Hakkarainen, M., Albertsson, A., 2004. Environmental degradation of polyethylene. Adv. Polym. Sci. 169, 177–199.

Ranby, B., Lucki, J., 1980. New aspects of photodegradation and photooxidation of polystyrene. Pure Appl. Chem. 52, 295–303.

Gewert, B., Plassmann, M.M., MacLeod, M., 2015. Pathways for degradation of plastic polymers floating in the marine environment. Environ. Sci. Process. Impacts 17, 1513–1521.

Andrady, A.L., 2015. Persistence of plastic litter in the oceans. In: Bergmann, M., Gutow, L., Klages, M. (Eds.), Marine Anthropogenic Litter. Springer, pp. 57–72.

Powers, L.C., Brandes, J.A., Stubbins, A., Miller, W.L., 2017. MoDIE: moderate dissolved inorganic carbon (DI^{13}C) isotope enrichment for improved evaluation of DIC photochemical production in natural waters. Mar. Chem. 194, 1–9.

Enders, K., Lenz, R., Stedmon, C.A., Nielsen, T.G., 2015. Abundance, size and polymer composition of marine microplastics ≥10 μm in the Atlantic Ocean and their modelled vertical distribution. Mar. Pollut. Bull. 100, 70–81.

Gewert, B., Plassmann, M., Sandblom, O., MacLeod, M., 2018. Identification of chain scission products released to water by plastic exposed to ultraviolet light. Environ. Sci. Tech. Let. 5, 272–276.

Royer, S., Ferrón, S., Wilson, S.T., Karl, D.M., 2018. Production of methane and ethylene from plastic in the environment. PLoS One 13, e200574.

Lambert, S., Wagner, M., 2016. Characterisation of nanoplastics during the degradation of polystyrene. Chemosphere 145, 265–268.

Romera-Castillo, C., Pinto, M., Langer, T.M., Álvarez-Salgado, X.A., Herndl, G.J., 2018. Dissolved organic carbon leaching from plastics stimulates microbial activity in the ocean. Nat. Commun. 9, 1430.

Dittmar, T., 2014. A. Stubbins. 12.6-dissolved organic matter in aquatic systems. In: Hollaand, H.D., Turekian, K.K. (Eds.), Treatise on Geochemistry, 2nd ed. Elsevier, Oxford, UK, pp. 125–156.

Moran, M.A., Kujawinski, E.B., Stubbins, A., Fatland, R., Aluwihare, L.I., Buchan, A., Crump, B.C., Dorrestein, P.C., Dyhrman, S.T., Hess, N.J., Howe, B., Longnecker, K., Medeiros, P.M., Niggemann, J., Obernosterer, I., Repeta, D.J., Waldbauer, J.R., 2016. Deciphering ocean carbon in a changing world. Proc. Natl. Acad. Sci. U.S.A. 113, 3143–3151.

Erni-Cassola, G., Zadjelovic, V., Gibson, M.I., Christie-Oleza, J.A., 2019. Distribution of plastic polymer types in the marine environment; A meta-analysis. J. Hazard. Mater. 369, 691–698.

Stubbins, A., Dittmar, T., 2012. Low volume quantification of dissolved organic carbon and dissolved nitrogen. Limnol. Oceanogr-Meth. 10, 347–352.

Morét-Ferguson, S., Law, K.L., Proskurowski, G., Murphy, E.K., Peacock, E.E., Reddy, C.M., 2010. The size, mass, and composition of plastic debris in the western North Atlantic Ocean. Mar. Pollut. Bull. 60, 1873–1878.

Stubbins, A., Niggemann, J., Dittmar, T., 2012. Photo-lability of deep ocean dissolved black carbon. Biogeosciences 9, 1661–1670.

Andrady, A.L., Pegram, J.E., Searle, N.D., 1996. Wavelength sensitivity of enhanced photodegradable polyethylenes, ECO, and LDPE/MX. J. Appl. Polym. Sci. 62, 1457–1463.

Zhang, Z., Hu, X., Luo, Z., 1996. Wavelength sensitivity of photooxidation of polypropylene. Polym. Degrad. Stabil. 51, 93–97.

Stubbins, A., Mann, P.J., Powers, L., Bittar, T.B., Dittmar, T., McIntyre, C.P., Eglinton, T.I., Zimov, N., Spencer, R.G.M., 2017. Low photolability of yedoma permafrost dissolved organic carbon. J. Geophys. Res. Biogeosci. 122, 200–211.

Sharp, J.H., 1974. Improved analysis for "particulate" organic carbon and nitrogen from seawater. Limnol. Oceanogr. 19, 984–989.

Corcoran, P.L., Biesinger, M.C., Grifi, M., 2009. Plastics and beaches: a degrading relationship. Mar. Pollut. Bull. 58, 80–84.

Rajakumar, K., Sarasvathy, V., Thamarai Chelvan, A., Chitra, R., Vijayakumar, C.T., 2009. Natural weathering studies of polypropylene. J. Polym. Environ. 17, 191–202.

Taylor, J., 1997. Propagation of uncertainties. In: Taylor, J. (Ed.), An Introduction to Error Analysis, the Study of Uncertainties in Physical Measurements, 2nd ed. University Science Books, pp. 45–79.

Spencer, R.G.M., Mann, P.J., Dittmar, T., Eglinton, T.I., McIntyre, C., Holmes, R.M., Zimov, N., 2015. A. Stubbins. Detecting the signature of permafrost thaw in Arctic rivers. Geophys. Res. Lett. 42, 2830–2835.

Spencer, R.G.M., Guo, W., Raymond, P.A., Dittmar, T., Hood, E., Fellman, J., Stubbins, A., 2014. Source and biolability of ancient dissolved organic matter in glacier and lake ecosystems on the Tibetan Plateau. Geochim. Cosmochim. Ac. 142, 64–74.

Holmes, R.M., McClelland, J.W., Raymond, P.A., Frazer, B.B., Peterson, B.J., Stieglitz, M., 2008. Lability of DOC transported by alaskan rivers to the Arctic Ocean. Geophys. Res. Lett. 3, L03402.

Redfield, A.C., 1934. On the Proportions of Organic Derivatives in Sea Water and Their Relation to the Composition of Plankton. James Johnstone Memorial Volume. University Press of Liverpool, pp. 176–192.

Gasol, J.M., Del Giorgio, P.A., 2000. Using flow cytometry for counting natural planktonic bacteria and understanding the structure of planktonic bacterial communities. Sci. Mar. 64, 197–224.

Brandon, J., Goldstein, M., Ohman, M.D., 2016. Long-term aging and degradation of microplastic particles: Comparing in situ oceanic and experimental weathering patterns. Mar. Pollut. Bull. 110, 299–308.

Eyheraguibel, B., Leremboure, M., Traikia, M., Sancelme, M., Bonhomme, S., Fromageot, D., Lemaire, J., Lacoste, J., Delort, A.M., 2018. Environmental scenarii for the degradation of oxo-polymers. Chemosphere 198, 182–190.

Kitidis, V., Stubbins, A.P., Uher, G., Upstill Goddard, R.C., Law, C.S., Woodward, E.M.S., 2006. Variability of chromophoric organic matter in surface waters of the Atlantic Ocean. DEEP-SEA RES. PT II 53, 1666–1684.

Mopper, K., Kieber, D.J., Stubbins, A., 2015. Marine photochemistry of organic matter: processes and impacts. In: Hansell, D., Carlson, C. (Eds.), Biogeochemistry of Marine Dissolved Organic Matter, 2nd ed. Academic Press, pp. 389–450.

Tidjani, A., 1997. Photooxidation of polypropylene under natural and accelerated weathering conditions. J. Appl. Polym. Sci. 64, 2497–2503.

Geuskens, G., David, C., 1979. Recent advances in the photo-oxidation of polymers. Pure Appl. Chem. 51, 2385–2393.

Carlsson, D.J., Garton, A., Wiles, D.M., 1976. Initiation of polypropylene photooxidation. 2. Potential processes and their relevance to stability. Macromolecules 9, 695–701.

Maximenko, N., Hafner, J., Niiler, P., 2012. Pathways of marine debris derived from trajectories of Lagrangian drifters. Mar. Pollut. Bull. 65, 51–62.

Lee, J., Lee, J.S., Jang, Y.C., Hong, S.Y., Shim, W.J., Song, Y.K., Hong, S.H., Jang, M., Han, G.M., Kang, D., Hong, S., 2015. Distribution and size relationships of plastic marine debris on beaches in South Korea. Arch. Environ. Con. Tox. 69, 288–298.

Sadri, S.S., Thompson, R.C., 2014. On the quantity and composition of floating plastic debris entering and leaving the Tamar Estuary. Southwest England. Mar. Pollut. Bull. 81, 55–60.

Sun, X., Liang, J., Zhu, M., Zhao, Y., Zhang, B., 2018. Microplastics in seawater and zooplankton from the Yellow Sea. Environ. Pollut. 242, 585–595.

Bittar, T.B., Vieira, A.A.H., Stubbins, A., Mopper, K., 2015. Competition between photochemical and biological degradation of dissolved organic matter from the cyanobacteria Microcystis aeruginosa. Limnol. Oceanogr. 60, 1172–1194.

Carlson, C.A., Giovannoni, S.J., Hansell, D.A., Goldberg, S.J., Parsons, R., Otero, M.P., Vergin, K., Wheeler, B.R., 2002. Effect of nutrient amendments on bacterioplankton production, community structure, and DOC utilization in the northwestern Sargasso Sea. Aquat. Microb. Ecol. 30, 19–36.